Atmos. Chem. Phys. Discuss., 13, 17053–17085, 2013
www.atmos-chem-phys-discuss.net/13/17053/2013/
doi:10.5194/acpd-13-17053-2013

Atmospheric Chemistry and Physics
Discussions
Open Access

The variability of methane, nitrous oxide and sulfur hexafluoride in Northeast India

A. L. Ganesan[1], A. Chatterjee[2], R. G. Prinn[1], C. M. Harth[3], P. K. Salameh[3], A. J. Manning[4], B. D. Hall[5], J. Mühle[3], L. K. Meredith[1], R. F. Weiss[3], S. O'Doherty[6], and D. Young[6]

[1]Center for Global Change Science, Massachusetts Institute of Technology, Cambridge, Massachusetts, USA
[2]Environmental Sciences Section, Bose Institute, Kolkata, India
[3]Scripps Institution of Oceanography, University of California San Diego, La Jolla, California, USA
[4]Atmospheric Dispersion Group, Met Office, Exeter, UK
[5]NOAA Earth System Research Laboratory, Boulder, Colorado, USA
[6]Atmospheric Chemistry Research Group, University of Bristol, Bristol, UK

Received: 16 May 2013 – Accepted: 13 June 2013 – Published: 27 June 2013

Correspondence to: A. L. Ganesan (aganesan@mit.edu)

Published by Copernicus Publications on behalf of the European Geosciences Union.

Abstract

High-frequency atmospheric measurements of methane (CH_4), nitrous oxide (N_2O) and sulfur hexafluoride (SF_6) from Darjeeling, India are presented from December 2011 (CH_4)/March 2012 (N_2O and SF_6) through February 2013. These measurements were made on a gas chromatograph equipped with a flame ionization detector and electron capture detector and were calibrated on the Tohoku University, the Scripps Institution of Oceanography (SIO)-98 and SIO-2005 scales for CH_4, N_2O and SF_6, respectively. The observations show large variability and frequent pollution events in CH_4 and N_2O mole fractions, suggesting significant sources in the regions sampled by Darjeeling throughout the year. In contrast, SF_6 mole fractions show little variability and only occasional pollution episodes, likely due to weak sources in the region. Simulations using the Numerical Atmospheric dispersion Modelling Environment (NAME) particle dispersion model suggest that many of the enhancements in the three gases result from the transport of pollutants from the densely populated Indo-Gangetic plains of India to Darjeeling. The meteorology of the region varies considerably throughout the year from Himalayan flows in the winter to the strong South Asian summer monsoon. The model is consistent in simulating a diurnal cycle in CH_4 and N_2O mole fractions that is present during the winter but absent in the summer and suggests that the signals measured at Darjeeling are dominated by large scale (~ 100 km) flows rather than local (< 10 km) flows.

1 Introduction

Methane (CH_4), nitrous oxide (N_2O) and sulfur hexafluoride (SF_6) are potent greenhouse gases that play a significant role in the climate system. Atmospheric CH_4 is the second largest contributor to anthropogenic radiative forcing after carbon dioxide (CO_2) at 0.48 W m^{-2} (Forster et al., 2007). The major sink for CH_4 is reaction with the hydroxyl radical (OH), resulting in an atmospheric lifetime of 12 yr (Forster et al., 2007).

Globally, a large fraction of CH_4 emissions are naturally occurring and primarily originate from wetlands but anthropogenic sources, which include rice paddies, ruminants and biomass burning, dominate with ∼ 60 % of the CH_4 budget (Chen and Prinn, 2006; Denman et al., 2007). In India, over 75 % of CH_4 emissions are from the agricultural sector through enteric fermentation and microbial processes in rice paddies (Indian Network for Climate Change Assessment, 2007). The peak in CH_4 emissions occurs during the wet season (June to September) when the majority of rice in South Asia is grown (Pathak et al., 2005).

N_2O is a powerful greenhouse gas and ozone-depleting substance. Based on current mole fractions, N_2O has the third largest anthropogenic radiative forcing (Forster et al., 2007). The main sink for N_2O occurs in the stratosphere where photolysis and reaction with $O(^1D)$ result in an atmospheric residence time of ∼ 114 yr (Forster et al., 2007). N_2O also plays a significant role in the chemistry of the ozone layer and is the primary source of stratospheric NO_x. Though its ozone-depletion potential (ODP) is low (0.017), its large atmospheric burden and long lifetime make N_2O the largest ODP-weighted emitter (Ravishankara et al., 2009). The principal sources of N_2O globally occur naturally from microbial processes in soils and in the ocean and these sources account for approximately 60 % of the budget. The remainder of emissions is anthropogenically emitted through the usage of fertilizers in agricultural soils, from biomass burning, sewage, transportation and other smaller sources (Denman et al., 2007). The dominant N_2O source in India is from fertilized soils in rice and wheat agriculture and comprises over 60 % of national emissions (Indian Network for Climate Change Assessment, 2007).

SF_6 is the most potent greenhouse gas regulated under the Kyoto Protocol with a 100 yr global warming potential of 22 800. Its lifetime of 3200 yr owes to the fact that destruction of SF_6 only occurs in the mesosphere, making it essentially inert on human timescales (Forster et al., 2007). Measurements of SF_6 from firn air have shown only a small pre-industrial concentration of 6×10^{-3} pmol mol^{-1}, suggesting that SF_6 is almost entirely anthropogenically emitted (Deeds et al., 2008). Emissions globally

ACPD
13, 17053–17085, 2013

and in India are largely from the electrical industry through leakage from high-voltage switchgear and during the maintenance and refill process (Niemeyer and Chu, 1992).

Global monitoring of atmospheric mole fractions has existed for several decades for CH_4 and N_2O and has been implemented in the past decade for SF_6 (Prinn et al., 2000; Dlugokencky et al., 2005; Hall et al., 2007). Global emissions for the three gases have been deduced in previous studies using data from global measurement networks. CH_4 emissions have been estimated to be between 500–600 Tg CH_4 yr^{-1} from 1996–2004 (Chen and Prinn, 2006; Bergamaschi et al., 2009). A recent increase in the growth rate of CH_4 was detected in 2007 following a decade of stability, and the cause of this increase remains unresolved but is speculated to result from changes in tropical emissions (Rigby et al., 2008; Dlugokencky et al., 2009; Bousquet et al., 2011). Global N_2O and SF_6 emissions have been estimated to be between 15.4–17.3 TgN yr^{-1} from 1997–2005 and 7.2–7.4 Gg yr^{-1} in 2008, respectively (Hirsch et al., 2006; Huang et al., 2008; Rigby et al., 2010; Levin et al., 2010).

Quantification of regional emissions using atmospheric measurements are less constrained than the global burden primarily because they require measurements that sample air masses containing regional pollution rather than measurements that sample the "background". Previous measurements in South Asia include low-frequency flask measurements and satellite observations. Between 1993–2002 and from 2009–present, flasks have been collected biweekly at a station in Cabo de Rama, India (Cape Rama) and measured for CH_4 and N_2O mole fraction at the Commonwealth Scientific and Industrial Research Organization (CSIRO) (Bhattacharya et al., 2009). Previous and ongoing satellite measurements include measurements by SCIAMACHY (SCanning Imaging Absorption SpectroMeter for Atmospheric CHartographY), AIRS (Atmospheric Infrared Sounder) and GOSAT (Greenhouse gases Observing SATellite) (Bergamaschi et al., 2009; Xiong et al., 2009; Parker et al., 2011). In Xiong et al. (2009), satellite retrievals of CH_4 showed a plume-like enhancement of CH_4 over South Asia during the monsoon, suggesting enhanced emissions and deep convection during this period. Samples collected by CARIBIC (Civil Aircraft for the Regular Investigation of the atmosphere Based on an Instrument Container) flights have also shown a similar monsoon plume (Schuck et al., 2010).

Of the many global emissions estimates for these gases, only a few studies have utilized atmospheric measurements from South Asia. In Bergamaschi et al. (2009), CH_4 emissions over Asia (including India, China and Southeast Asia) were estimated using SCIAMACHY retrievals with a CO_2 proxy and NOAA surface data at 128.4 $Tg\,yr^{-1}$. The study showed the large spatial and temporal variability in CH_4 source strength within India. However, satellite retrievals over India are often compromised in areas with frequent cloud cover and high aerosol optical depth (Parker et al., 2011). Retrievals based on CO_2 proxies may have additional uncertainties for India due to the sparsity of available CO_2 measurements in the region. The importance of including Cape Rama measurements from India in regional emissions estimates has been demonstrated in Huang et al. (2008). Inversions for N_2O emissions performed with Cape Rama data showed significant error reduction over the case when Indian measurements were not included and also showed that large spatial covariances exist between emissions derived for South Asia and other regions without the use of these measurements. The results of this study found South Asian N_2O emissions (region encompassing India, the Middle East and portions of China) to be 0.95 $TgN\,yr^{-1}$ from 2002–2005. Total SF_6 emissions for all non-UNFCCC (United Nations Framework Convention on Climate Change) Asian countries were estimated to be 4.1 $Gg\,yr^{-1}$ in 2008 (Rigby et al., 2010).

Due the importance of using measurements from South Asia in estimating emissions from the region, measurements of CH_4, N_2O and SF_6 have been collected from Darjeeling, India from December 2011 (CH_4)/March 2012 (N_2O and SF_6) through February 2013 and are currently ongoing. These measurements comprise a pilot study for the Darjeeling station, which is the first to measure these three gases in situ in India and with instrumentation sampling at high-frequency, resulting in measurements that could provide important constraints for top-down emissions estimation.

ACPD
13, 17053–17085, 2013

2 Experimental methods

A fully automated, custom-built sampling system was developed and integrated with a gas chromatograph (GC, Agilent Technologies, Santa Clara, CA, model 6890N) equipped with a flame ionization detector (FID) and micro electron capture detector (µECD, henceforth referred to as ECD) to measure CH_4 (FID), N_2O and SF_6 (ECD). Development of the instrument was based on similar designs by Prinn et al. (2000), Hall et al. (2007, 2011), and Dlugokencky et al. (2005). Full details of the instrument design and characterization are provided in the Supplement. Analysis time for each sample has varied between ten and twelve minutes during this study.

Though measurement on the FID and ECD are performed simultaneously, each channel is discussed separately. Carrier gas for the FID is nitrogen at a purity of 99.999 %. Hydrogen fuel gas at 99.999 % purity is supplied to the FID at 60 mL min^{-1} along with zero air from a pure air generator equipped with a CH_4 reactor (Aadco Instruments Inc, Cleves, OH, model 737-1A) at 275 mL min^{-1}. After the FID sample loop has equilibrated to ambient pressure, the sample is injected through a 10-port 2-position backflush valve (BFV) onto a HayeSep Q 100/120 pre-column (3′, 1/8″ OD) and main-column (6′, 1/8″ OD). After CH_4 has eluted off the pre-column, the BFV is switched to the backflush position at which time the pre-column is backflushed and CH_4 continues through the main-column to the FID. The column and backflush flow rates are 40 mL min^{-1} and 20 mL min^{-1}, respectively. The column temperature is held isothermally at 85 °C and the detector is maintained at 190 °C.

For the ECD channel, carrier gas is a 10 % CH_4 in argon mixture (P-10) at a purity of 99.995 % (relative to the mixture). The sample is injected after equilibration to ambient pressure through a 10-port 2-position BFV onto a Porapak Q 80/100 pre-column (1′, 3/16″ OD) and main-column (2′, 3/16″ OD), where N_2O and SF_6 are separated from air. After oxygen elutes from these columns, it is “heart-cut” out to the vent, upon which the BFV is switched so that the pre-column is backflushed while N_2O and SF_6 continue through the main-column onto a third Molecular Sieve 5Å 40/60 post-column. On the post-column, the order of elution of N_2O and SF_6 is reversed so that SF_6 is detected before the much larger N_2O peak in order to improve the SF_6 response. N_2O co-elutes with CO_2 on this post-column, but care is taken to ensure that the N_2O response is not affected by variations in ambient CO_2. This third post-column is contained in a custom-built oven that is controlled and modulated by one of the heated zones on the GC. The pre- and main- columns are maintained at 85 °C for consistency with the FID system, the post-column is held at 180 °C and the ECD detector temperature at 340 °C. Column flow is 35 mL min^{-1} during the heart-cut, increased to 40 mL min^{-1} through the post-column and is 30 mL min^{-1} during backflush. P-10 exhaust is vented outside the lab to prevent any accidental contamination of CH_4 onto the FID system.

Measurements were calibrated using a dry compressed air standard filled in an aluminum cylinder (Scott Marrin, Riverside, CA) at the Scripps Institution of Oceanography (SIO) in July 2012. The cylinder was first passivated with air for approximately a week and then evacuated and re-filled. The standard was calibrated to values of 1835.01 ± 1.16 nmol mol^{-1}, 324.60 ± 0.09 nmol mol^{-1}, and 7.55 ± 0.04 pmol mol^{-1} for CH_4, N_2O and SF_6, respectively, using the Advanced Global Atmospheric Gases Experiment (AGAGE) Multi-Detector system (for CH_4 and N_2O) and the AGAGE "Medusa" GC-Mass Spectrometer system (for SF_6). CH_4, N_2O and SF_6 were calibrated on the Tohoku University, SIO-98 and SIO-2005 scales, respectively (Prinn et al., 2000; Miller et al., 2008). Standard and air samples were measured alternately.

Due to the high fill pressure and large volume of the cylinder, enough standard gas is available in the cylinder to calibrate the instrument for three years. Studies using dry standards filled in aluminum cylinders have been used widely and have shown no significant drift for each of the three gases over the timeframe of this study (Dlugokencky et al., 2005; Hall et al., 2007, 2011). To determine any possible drift in the standard, the ratios of the standard and two other calibrated cylinders have been monitored. No drift within the repeatability of the instrument has been observed for the three gases.

On this system, median 1σ repeatability achieved for the three gases over the period of study was 1.2 nmol mol^{-1} (CH_4), 0.17 nmol mol^{-1} (N_2O) and 0.03 pmol mol^{-1} (SF_6),

ACPD
13, 17053–17085, 2013

which lie within the ranges typically achieved for these gases at AGAGE stations (Prinn et al., 2000; Cunnold et al., 2002; Huang et al., 2008; Rigby et al., 2010).

Meteorological measurements were collected at the station for air temperature, barometric pressure, wind speed and direction, solar radiation and precipitation using sensors that were installed prior to this study in 2010. Components of the meteorological station are found in the Supplement. The measurements used in this study are one minute averages of 10 Hz data.

3 Field site

The field site selected for this study is located in Darjeeling, India, a high-altitude hill station in the eastern Himalayas (27°02′ N, 88°15′ E, 2194 m a.s.l., Chatterjee et al., 2010). Instrumentation is housed at the National Facility of Astroparticle Physics and Space Science of the Bose Institute. Darjeeling has population of ~ 100 000 and has developed on the northwest facing slope of a northeast-southwest oriented ridge (Fig. 1). The main town center in Darjeeling is located at approximately 2000 m a.s.l., 200 m below the station and 250 m below the ridgetop. It is located ~ 50 km north of the densely populated Indo-Gangetic plains. The measurement station is located in a relatively unpopulated portion of Darjeeling. There is one road that leads to the Bose Institute shortly after which the road ends resulting in very little vehicular traffic on this road.

The slope below Darjeeling contains several tea plantations, where synthetic nitrogen fertilizers are used seasonally and could contribute to a local source of N_2O. Wood biomass burning is prevalent throughout the mountain region and mainly during the winter season, which may contribute to local sources of CH_4 and N_2O. Additionally, there may be small natural gas sources from fuel, another potential local influence on CH_4. Vehicular emissions also exist, mainly from tourist vehicles which operate predominantly on diesel fuel, though the contribution to CH_4 and N_2O is thought to be small. Local sources of SF_6 are expected to be low. The nearest high-voltage power

ACPD
13, 17053–17085, 2013

substation is located in Ghoom, approximately 10 km away from Darjeeling but could be a potential source of SF_6.

The inlet line to the instrument was installed approximately midway on a ten meter tower that was built on the roof of a four-story building. Meteorological sensors were mounted above the instrument inlet at the top of the tower. Details of the inlet setup are provided in the Supplement.

4 Transport model

A transport model was used to diagnose important signals in the trace gas data and to characterize the meteorology of the site. The UK Met Office's Numerical Atmospheric dispersion Modelling Environment version 3 (NAME) is a Lagrangian particle dispersion model used to simulate atmospheric transport (Ryall and Maryon, 1998; Jones et al., 2007) and has been used extensively for similar applications and at various sites (Manning et al., 2011, 2003; O'Doherty et al., 2004; Reimann et al., 2005). NAME calculates transport by following a large number of particles "backwards" in time from release at the measurement site. The particles are advected by three-dimensional meteorological fields supplied by a Numerical Weather Prediction (NWP) model but also include additional turbulent and low-frequency meandering motions that are simulated by a random-walk formulation (Morrison and Webster, 2005). Chemistry, wet and dry deposition and radioactive decay can be included but owing to the long lifetimes of the gases being studied here and the length of the back trajectories, particles were assumed to be inert. The computational domain used for the model runs over Darjeeling was from 5–50° N, 50–120° E, covering India, China, Southeast Asia, and part of the Middle East and up to 19 km vertically. Particles were released from the Darjeeling station (27°02′ N, 88°15′ E) at a release height between 450–550 m a.g.l. and were released randomly throughout this 100 m column. The particle release height was chosen as a compromise between the true station height (2194 m a.s.l.) and the height of the station in the model (1340 m a.s.l.). A release height between these two station

ACPD
13, 17053–17085, 2013

heights is typically chosen at mountain sites (Brunner et al., 2012; Tuzson et al., 2011). Particles were released continuously at a rate of 20 000 particles hr^{-1} at a mass of 1 $g\,s^{-1}$ for each three hour period and tracked backwards for 30 days.

NWP meteorological fields from the Met Office's Unified Model (UM) were used to drive NAME. Model simulations utilized the UM South Asian Model (SAM), which is available from 2010 onwards for the South Asian domain at 0.11° horizontal resolution, for 70 vertical levels and at three-hour temporal resolution. Seven days after release, at which time particles are assumed to have left the Himalayas, or if particles have left the SAM domain prior to this time, the UM's global meteorology at 0.352° × 0.234° resolution was used. The model time step in all simulations was five minutes.

NAME outputs "air histories" or the influence of surface emissions on the measured concentrations at the station and directly provides the sensitivity of a measurement in Darjeeling to emissions from the domain. Air histories were created at 0.352° × 0.234° resolution for a 0–100 m a.g.l. vertical level every three hours.

5 Results

Measurements of CH_4, N_2O and SF_6 mole fractions from Darjeeling, India are presented for the period from December 2011 for CH_4 and March 2012 for N_2O and SF_6 through February 2013. Meteorological measurements and air histories from the period are used to explain the signals observed in the mole fraction measurements.

5.1 Air histories and meteorology

Monthly median air history maps are shown for each season and indicate the regions sampled by Darjeeling (Fig. 2). January air histories show surface influence from both east and west of the station, indicating that air from both sides of the site is sampled after particles are released from Darjeeling. This likely results from diurnal changes in wind direction caused by thermally-driven slope winds in the mountains. During the

ACPD
13, 17053–17085, 2013

Greenhouse gas measurements from Northeast India

A. L. Ganesan et al.

day, air flows from the plains to the mountains and locally upslope, while at night air largely descends from the mountains down to the plains and locally downslope. During the winter, the greatest sensitivity to the surface is localized to the Himalayan region. In April, the east and west "lobes" caused by diurnal winds are still seen but southerly winds are additionally present. In these 30 day integrated maps, this suggests that a fraction of particles move with the diurnal winds and a fraction are carried by the larger-scale flow. In the summer period, only the dominant summer monsoon flow is observed. During the monsoon, the large temperature contrast between the Asian landmass and Indian Ocean results in a surface low pressure system over India (Hoskins and Rodwell, 1995). A strong southwesterly flow (known as the Southwest Monsoon) brings moisture-laden air from the ocean to the continent and results in intense precipitation over South Asia. This summer monsoon is also characterized by strong convection over the heating landmass that can transport pollutants to the upper troposphere (Schuck et al., 2010; Xiong et al., 2009). In October following the summer monsoon, the "lobes" return and air histories are similar to those seen in January. The seasonal differences in the air histories shows the different flows captured between winter and summer and suggests that Darjeeling samples air masses from several regions of South Asia throughout the year.

To asses the ability of the UM to reproduce flows at the site as well as to understand the origin of air masses sampled at the site, observed and modeled wind speeds and wind directions are compared using wind roses (Fig. 3). UM modeled winds are shown at 500 m a.g.l., which is the mid-point particle release height used in the model.

Horizontal wind speeds at Darjeeling maximize in April (not shown) during the pre-monsoon period and minimize in July when vertical motion is strong in the Himalayas. Wind speeds are almost always larger in the 500 m a.g.l. model winds than in the 15 m a.g.l. observed winds because surface friction is less significant at this height in the model and could contribute to errors in the derived air histories.

In January, 500 m a.g.l. modeled and observed winds at 15 m a.g.l. show good agreement in wind direction. Air flow is southerly during the day and northeasterly at night,

ACPD
13, 17053–17085, 2013

which is consistent with the direction of plains-to-mountain winds. Upslope and downslope winds local to the Darjeeling ridge, which is oriented towards the northeast, would result in observed and modeled diurnal winds that are oriented to the southeast and northwest, respectively if the flow being captured was a local process. This diurnal shift in wind direction, which is well-captured by the model, is responsible for the "lobes" seen in the winter air history maps (Fig. 2). In July, the diurnal cycle in wind direction is not significant and this lack of diurnal cycle is reproduced in the model as well. Both the model and observations show a consistent southeasterly wind direction at this time, resulting from air masses that originate from the southwest but first pass over the Bay of Bengal before reaching Darjeeling from the southeast. The consistency between the model and observations suggest that the air sampled at Darjeeling is representative of the "large-scale" flows of the region rather than the local mesoscale flows.

Sensible heat flux is a measure of the heat transferred between the surface and atmosphere and can be indicative of the prominence of slope winds. Sensible heat flux from the UM was averaged into diurnal values for January 2012 and July 2012 and used to diagnose seasonal variability in the diurnal cycle (Supplement). While sensible heat flux in both months maximize at $\sim$ 12 p.m., It was found that the wintertime diurnal sensible heat flux was considerably larger than that of the summer. This could occur for several reasons: (1) winter days in Darjeeling are very clear and are generally cloud-free, resulting in more solar radiation reaching the surface; (2) the winter is dry while the summer is humid, which results in solar radiation absorbed by the surface to be converted to latent heat flux rather than to sensible heat flux; (3) there is a dominant synoptic flow in the summer, which may be stronger than the diurnal flows.

5.2 Trace gas measurements

Darjeeling intercepts air with surrounding "regional" pollution, air that characterizes the "background" and occasionally air with "local" influence. These three types of signals are defined broadly as the signal characterizing emissions from South Asia, the signal pertaining to well-mixed air masses and the signal characterizing local Darjeeling

ACPD
13, 17053–17085, 2013

emissions. The measurement time series from December 2011 through February 2013 for the three gases at Darjeeling are compared with "pollution-removed" monthly mean mole fractions from several AGAGE stations (Fig. 4).

SF_6 is discussed first as its mole fractions at Darjeeling generally vary slowly with time and pollution episodes are infrequent. Though Darjeeling lies approximately halfway latitudinally between Ireland and Barbados, the signal is most similar in magnitude to that of Ragged Point, Barbados. This could result from the Himalayas serving as a barrier to the transport of high latitude air to Darjeeling as well as from the fact that Darjeeling is at a higher altitude than Mace Head, Ireland. The magnitude of pollution events measured at Darjeeling is smaller than those seen at polluted stations such as Gosan, South Korea, suggesting that sources of SF_6 near Darjeeling are weaker or farther away than those sampled at Gosan (Rigby et al., 2010). It is assumed that the SF_6 record is indicative of Darjeeling's place within the global latitudinal gradient if few regional sources are present. In contrast, CH_4 and N_2O mole fractions are significantly elevated over the assumed background level, and are even further elevated over Mace Head levels. This suggests that there are strong regional sources present that almost always enhance CH_4 and N_2O over the background, though at occasional times during the winter, their mole fractions exhibit excursions down to Ragged Point, Barbados levels. These low excursions could imply either that background air is sampled occasionally or that cleaner mid to upper tropospheric air is being sampled during times of subsidence.

The monthly mean CH_4 mole fraction and 1σ variability in January 2012 and July 2012 are 1929.2 (55.7) and 1923.6 (64.8) $\mathrm{nmol\,mol^{-1}}$, respectively, values which are similar for both seasons. While it is expected that CH_4 and N_2O emissions peak in summer when wet season production of the two gases is greatest, the influence of the background mole fractions serves to compensate for the effect of increased emissions. In winter, air histories show transport of northern hemispheric air into India. In summer, the Southwest Monsoon results in the transport of southern hemispheric air into India with lower background content of CH_4, N_2O and SF_6.

ACPD
13, 17053–17085, 2013

Greenhouse gas measurements from Northeast India

A. L. Ganesan et al.

A fast Fourier transform (FFT) was applied to each month of CH_4 data (for months when continuous data was available for the majority of the month) to diagnose the dominant timescales of variability in each month (Fig. 5). A mean and linear trend were first removed and data padded with zeros to reach an integral power of 2 number of data points following Thoning et al. (1989). Because of data gaps in the full dataset, the FFT was not applied to the entire time series. Excluding trends in the monthly data, the dominant timescale of variability in the January measurements is diurnal, while in July, the diurnal signal is small. In July, the dominant variability is from synoptic-scale events on timescales of the order of a week. High-frequency variability (i.e., shorter than a day) is greater in July than in January, suggesting variability in the air masses sampled during the highly convective monsoon period, variability in source strength as emissions from rice paddies could be episodic or greater local influence from nearby Darjeeling sources. A similar spectrum is seen in N_2O measurements, while SF_6 shows greater high-frequency variability in all seasons owing to its lower measurement repeatability and no diurnal cycle in any season (Supplement).

5.2.1 Pollution events

CH_4 and N_2O generally exhibit concurrent enhancements in their mole fractions. As the CH_4 and N_2O measurement systems only share common sampling, it is unlikely that measurement artifacts would lead to these enhancements, suggesting that emissions sources for the two gases in the regions sampled by Darjeeling are generally co-located. Though enhancements are concurrent, over the course of the study the ratio of the two gases does not remain constant. Correlation coefficients, r, between CH_4 and N_2O and between CH_4 and SF_6 were computed for winter and summer periods and are provided in the Supplement.

CH_4 and N_2O show greater correlation during the winter than during the summer and is 0.90 for the period from December 2012 through February 2013 and 0.63 from June through August 2012 (both significant on a 95 % confidence level according to a t test). Because the timing of events are concurrent (in the winter, the enhancements

ACPD
13, 17053–17085, 2013

are largely diurnal), this suggests that the temporal distribution of emissions of the two gases are similar during the winter. In the summer, the simultaneous enhancements in mole fractions but lower correlation coefficient suggests a different temporal distribution of emissions during the period. Emissions of CH_4 and N_2O from rice paddies and fertilized soils, respectively, have been found not to occur simultaneously during the summer monsoon period, as fertilizer application occurs at specific times over the growing season (Pathak et al., 2005; Schuck et al., 2010). The lower correlation could also result from a different distribution of local emissions of the two gases, which is more prominent in the summer when the high-frequency component of variability is more significant.

Enhancements between CH_4 (or N_2O) and SF_6 are not always simultaneous, which reflects a different source distribution for the two gases, assuming that SF_6 emissions are constant. The correlation coefficient between CH_4 and SF_6 is 0.22 for the period from December 2012 through February 2013 and 0.59 for June through August 2012 (both significant). The low correlation in winter results from the presence of a prominent CH_4 diurnal cycle but lack of SF_6 diurnal cycle. In summer, neither gas has a significant diurnal cycle and a larger correlation is derived.

The role of transport in producing enhancements in mole fractions is discussed for each season (excluding spring when only one month of data was available). CH_4 measurements were first averaged into six hourly values in order to smooth the data and minimize the influence of short duration pollution on this analysis. Average air histories corresponding to the times that measurements are 1σ above the mean of the period and for times that they are 1σ below the mean were derived. The difference between the two was computed to show the changes in air histories that are likely to be responsible for the observed signals (Figs. 6–8, unsmoothed data shown). At times when CH_4 mole fractions are enhanced during the winter, Darjeeling samples a larger extent of the Himalayan region and there is greater sensitivity to the surface. In summer, the air histories corresponding to measurements that are enhanced show greater sensitivity to northern India while those corresponding to measurements that are low show

ACPD
13, 17053–17085, 2013

greater sensitivity to southern India. The majority of CH_4 and N_2O emissions occur in the highly populated Indo-Gangetic plains of northern India (Fig. 1), (Patra et al., 2011; Huang et al., 2008, and references therein). In autumn, as the meteorology transitions from the summer monsoon flow to the winter Himalayan flow, differences in air histories between enhanced and low mole fractions are attributable to both types of flows. As enhancements between CH_4 and N_2O are typically concurrent, similar results are derived for N_2O.

An analysis of transport in producing SF_6 enhancements shows that the two events from August and September occur when air masses sampled at Darjeeling come from Eastern India and Southeast Asia (shown in Supplement), suggesting the possibility of new SF_6 sources in that region that are not included in the Emissions Database for Global Atmospheric Research (EDGAR) version 4.2 (JRC/PBL, 2011). Several SF_6 enhancements are observed in the winter. The air histories associated with these winter enhancements show small differences in the areas of the Himalayas that are sampled relative to measurements that are not enhanced but do not show a consistent pattern. As the number of SF_6 pollution events measured during the year are small relative to the number of pollution events in CH_4 and N_2O, these results could be biased toward these few events.

5.2.2 Diurnal cycle

The diurnal cycle is a prominent feature of the measured signal during the winter. Median CH_4 diurnal cycles (N_2O and SF_6 in the Supplement) over different seasons are compared with model-generated diurnal cycles for the same periods (Fig. 9). Simulated CH_4 mole fractions were generated using constant monthly emissions fields (Patra et al., 2011, scenario CH_4_CTL_E4 and references therein). Mole fractions were first detrended by subtracting the median value of each running twenty-four hour period from either the measurement or simulated time series. The median was chosen to minimize the effect of outliers. Variability in both the observed and simulated diurnal cycles are shown as the 16th and 84th percentile values of the month. The size and

Discussion Paper | Discussion Paper | Discussion Paper | Discussion Paper |

ACPD

13, 17053–17085, 2013

variability of the simulated diurnal cycles are dependent on the magnitude of emissions and particle release height in the model.

A diurnal cycle in CH_4 and N_2O mole fractions is observed during the winter but is not significant during the summer. During the winter, mole fractions maximize in the afternoon and minimize at night, which is consistent with diurnal profiles of wind direction (upslope from plains during the day) and wind speed (maximizes at ~ 3 p.m.) in the mountain system. The model-reproduced CH_4 diurnal cycle matches the wintertime phase, with a maximum in both the observed and modeled mole fractions between 3–5 p.m. The agreement of the phase of the diurnal cycle between model and measurements suggests that the underlying mechanism stems from a large-scale flow. Progressive removal of emissions from a growing radius around the site show that the diurnal cycle is preserved in the simulation even when emissions are removed up to 100 km away and confirms that the flow being modeled is a large-scale plains-to-mountain flow.

Two peaks are observed throughout the year in the diurnal cycles, with one peak occurring between 7–9 a.m. and the second peak between 3–5 p.m. This timing of the morning peak also shifts throughout the year, which is consistent changes in sunrise time throughout the year. The prominence of the morning peak changes from winter to summer. While the magnitude of the median morning peak signal remains similar, variability in the diurnal cycle grows from winter to summer. This peak may be a result of the ventilation of pollutants from a stable night-time inversion layer up to the site. The morning peak is a feature that is not captured in this setup of NAME, suggesting that boundary layer processes occurring local to the Darjeeling slope are not captured at this resolution. The height of release of the model particles may also contribute to this mismatch as it may be a near-surface phenomena. This type of double-peak is often seen in "urban pollutants" such as carbon monoxide, where morning and evening rush hours lead to elevated mole fractions (Panday and Prinn, 2009). However, vehicular emissions are not large sources of CH_4 and it is thought that this feature is caused mainly by radiative effects rather than by a variable emissions signal.

ACPD
13, 17053–17085, 2013

N_2O and SF_6 diurnal cycles are shown in the Supplement. Small differences are seen between CH_4 and N_2O diurnal cycles in their monthly variability but the general features are consistent, further supporting the radiative effects argument. An SF_6 diurnal cycle is not observed in any season, suggesting that sources near the Himalayas are too weak to create a diurnal signal that can be seen within the measurement repeatability.

6 Summary and conclusions

The first high-frequency measurements of CH_4, N_2O and SF_6 from India are presented from December 2011 (CH_4)/March 2012 (N_2O and SF_6) through February 2013, which represent a significant contribution to data from the region. While SF_6 mole fractions generally exhibit a slowly-varying background signal suggesting weak sources in the area, CH_4 and N_2O are often polluted and have enhanced mole fractions over the assumed background level. Due to the largely polluted air masses sampled for CH_4 and N_2O throughout the year and the high-frequency sampling of the instrumentation, these data can be used to verify national-scale emissions from South Asia.

The ability of the transport model to simulate transport at the site shows that the measurements at Darjeeling are representative of the "large-scale" transport of pollutants. While January and July monthly mean mole fractions of CH_4 are similar, the air histories of measurements during the two seasons are considerably different. In winter, air histories reflect a sensitivity to emissions from the Himalayan region and a significant diurnal cycle in CH_4 and N_2O mole fractions is both observed and simulated. In contrast with the winter, the summer monsoon flow is predominantly southwesterly throughout the summer period, resulting in high surface sensitivity to India and Bangladesh but also the transport of southern hemispheric background air.

Many of the enhancements seen in the three gases have been diagnosed as the large-scale transport of pollutants from source regions to Darjeeling. During the summer, many pollution events for the three gases can be explained by transport from the

Indo-Gangetic plains of northern India and some SF_6 events are shown to result from transport from Southeast Asia. CH_4 and N_2O enhancements observed during the winter occur when surface sensitivity is greater over a larger extent of the Himalayas. SF_6 wintertime pollution events are measured but their air histories show a less consistent pattern than in CH_4 and N_2O, likely due to the small SF_6 sources within the Himalayas.

Supplementary material related to this article is available online at: http://www.atmos-chem-phys-discuss.net/13/17053/2013/ acpd-13-17053-2013-supplement.zip.

Acknowledgements. We are grateful to Mrs. Yashodhara Yadav (Bose Institute) for her work in Darjeeling and for her dedicated and meticulous work in operating the instrument. We additionally thank Sibaji Raha, Sanjay Ghosh, Soumendra Singh and D. K. Roy (Bose Institute) for their tremendous efforts in maintaining site infrastructure and coordinating logistics for this project. We also wish to thank Adam Cox, Tim Arnold and Stephanie Mumma (Scripps Institution of Oceanography, SIO) for all the help they have provided with standards. This work was funded by the MIT Center for Global Change Science Director's Fund, the MIT Joint Program on the Science and Policy of Global Change, the Martin Family Society of Fellows for Sustainability, the MIT Energy Initiative, MIT International Science and Technology Initiatives and funding from NASA grant NNX11AF17G to MIT supporting the Advanced Global Atmospheric Gases Experiment (AGAGE). Funding for Mace Head, Ireland (MHD) and Ragged Point, Barbados (RPB) stations are from the NASA grant to MIT, Defra (MHD) and NOAA contract RA133R09CN0062 (RPB). Funding for Cape Matatula, American Samoa (SMO) is from NASA grant NNX07AE87G to SIO and the NASA grant to MIT.

References

Bergamaschi, P., Frankenberg, C., Meirink, J. F., Krol, M., Villani, M. G., Houweling, S., Dentener, F., Dlugokencky, E. J., Miller, J. B., Gatti, L. V., Engel, A., and Levin, I.: Inverse model-

ACPD
13, 17053–17085, 2013

Greenhouse gas measurements from Northeast India

A. L. Ganesan et al.

ing of global and regional CH_4 emissions using SCIAMACHY satellite retrievals, J. Geophys. Res., 114, D22301, doi:10.1029/2009JD012287, 2009. 17056, 17057

Bhattacharya, S. K., Borole, D. V., Francey, R. J., Allison, C. E., Steele, L. P., Krummel, P., Langenfelds, R., Masarie, K. A., Tiwari, Y. K., and Patra, P. K.: Trace gases and CO_2 isotope records from Cabo de Rama, India, Curr. Sci. India, 97, 1336–1344, 2009. 17056

Bousquet, P., Ringeval, B., Pison, I., Dlugokencky, E. J., Brunke, E.-G., Carouge, C., Chevallier, F., Fortems-Cheiney, A., Frankenberg, C., Hauglustaine, D. A., Krummel, P. B., Langenfelds, R. L., Ramonet, M., Schmidt, M., Steele, L. P., Szopa, S., Yver, C., Viovy, N., and Ciais, P.: Source attribution of the changes in atmospheric methane for 2006–2008, Atmos. Chem. Phys., 11, 3689–3700, doi:10.5194/acp-11-3689-2011, 2011. 17056

Brunner, D., Henne, S., Keller, C. A., Reimann, S., Vollmer, M. K., O'Doherty, S., and Maione, M.: An extended Kalman-filter for regional scale inverse emission estimation, Atmos. Chem. Phys., 12, 3455–3478, doi:10.5194/acp-12-3455-2012, 2012. 17062

Chatterjee, A., Adak, A., Singh, A. K., Srivastava, M. K., Ghosh, S. K., Tiwari, S., Devara, P. C. S., and Raha, S.: Aerosol chemistry over a high altitude station at northeastern Himalayas, India., PloS one, 5, e11122, doi:10.1371/journal.pone.0011122, 2010. 17060

Chen, Y.-H. and Prinn, R. G.: Estimation of atmospheric methane emissions between 1996 and 2001 using a three-dimensional global chemical transport model, J. Geophys. Res., 111, D10307, doi:10.1029/2005JD006058, 2006. 17055, 17056

Cunnold, D. M., Steele, L. P., Fraser, P. J., Simmonds, P. G., Prinn, R. G., Weiss, R. F., Porter, L. W., O'Doherty, S. J., Langenfelds, R. L., Krummel, P. B., Wang, H. J., Emmons, L. K., Tie, X. X., and Dlugokencky, E. J.: In situ measurements of atmospheric methane at GAGE/AGAGE sites during 1985–2000 and resulting source inferences, J. Geophys. Res., 107, doi:10.1029/2001JD001226, 2002. 17060

Deeds, D. A., Vollmer, M. K., Kulongoski, J. T., Miller, B. R., Mühle, J., Harth, C. M., Izbicki, J. A., Hilton, D. R., and Weiss, R. F.: Evidence for crustal degassing of CF_4 and SF_6 in Mojave Desert groundwaters, Geochim. Cosmochim. Ac., 72, 999–1013, doi:10.1016/j.gca.2007.11.027, 2008. 17055

Denman, K., Brasseur, G., Chidthaisong, A., Ciais, P., Cox, P., Dickinson, R., Hauglustaine, D., Heinze, C., Holland, E., Jacob, D., Lohmann, U., Ramachandran, S., da Silva Dias, P., Wofsy, S., and Zhang, X.: Couplings between changes in the climate system and biogeochemistry, in: Climate Change 2007: The Physical Science Basis, Contribution of Working Group I to the Fourth Assessment Report of the Intergovernmental Panel on Climate

Change, edited by: Solomon, S., Qin, D., Manning, M., Chen, Z., Marquis, M., Averyt, K. B., Tignor, M., and Miller, H. L., Cambridge University Press, Cambridge, UK and New York, NY, USA, 2007. 17055

Dlugokencky, E. J., Myers, R. C., Lang, P. M., Masarie, K. A., Crotwell, A. M., Thoning, K. W., Hall, B. D., Elkins, J. W., and Steele, L. P.: Conversion of NOAA atmospheric dry air CH_4 mole fractions to a gravimetrically prepared standard scale, J. Geophys. Res., 110, D18306, doi:10.1029/2005JD006035, 2005. 17056, 17058, 17059

Dlugokencky, E. J., Bruhwiler, L., White, J. W. C., Emmons, L. K., Novelli, P. C., Montzka, S. A., Masarie, K. A., Lang, P. M., Crotwell, A. M., Miller, J. B., and Gatti, L. V.: Observational constraints on recent increases in the atmospheric CH_4 burden, Geophys. Res. Lett., 36, L18803, doi:10.1029/2009GL039780, 2009. 17056

Forster, P., Ramaswamy, V., Artaxo, P., Berntsen, T., Betts, R., Fahey, D., Haywood, J., Lean, J., Lowe, D., Myhre, G., Nganga, J., Prinn, R., Raga, G., Schulz, M., and Dorland, R. V.: Changes in atmospheric constituents and in radiative forcing, in: Climate Change 2007: The Physical Science Basis, Contribution of Working Group I to the Fourth Assessment Report of the Intergovernmental Panel on Climate Change, edited by: Solomon, S., Qin, D., Manning, M., Chen, Z., Marquis, M., Averyt, K. B., Tignor, M., and Miller, H. L., Cambridge University Press, Cambridge, UK and New York, NY, USA, 2007. 17054, 17055

Hall, B. D., Dutton, G. S., and Elkins, J. W.: The NOAA nitrous oxide standard scale for atmospheric observations, J. Geophys. Res., 112, D09305, doi:10.1029/2006JD007954, 2007. 17056, 17058, 17059

Hall, B. D., Dutton, G. S., Mondeel, D. J., Nance, J. D., Rigby, M., Butler, J. H., Moore, F. L., Hurst, D. F., and Elkins, J. W.: Improving measurements of SF_6 for the study of atmospheric transport and emissions, Atmos. Meas. Tech., 4, 2441–2451, doi:10.5194/amt-4-2441-2011, 2011. 17058, 17059

Hirsch, A. I., Michalak, A. M., Bruhwiler, L. M., Peters, W., Dlugokencky, E. J., and Tans, P. P.: Inverse modeling estimates of the global nitrous oxide surface flux from 1998–2001, Global Biogeochem. Cy., 20, GB1008, doi:10.1029/2004GB002443, 2006. 17056

Hoskins, B. J. and Rodwell, M. J.: A model of the asian summer Monsoon, part I: the global scale, J. Atmos. Sci., 52, 1329–1340, doi:10.1175/1520-0469(1995)052<1329:AMOTAS>2.0.CO;2, 1995. 17063

Huang, J., Golombek, A., Prinn, R., Weiss, R., Fraser, P., Simmonds, P., Dlugokencky, E. J., Hall, B., Elkins, J., Steele, P., Langenfelds, R., Krummel, P., Dutton, G., and Porter, L.: Estimation of regional emissions of nitrous oxide from 1997 to 2005 using multinetwork measurements, a chemical transport model, and an inverse method, J. Geophys. Res., 113, D17313, doi:10.1029/2007JD009381, 2008. 17056, 17057, 17060, 17068

Indian Network for Climate Change Assessment: India: Greenhouse Gas Emissions 2007, Tech. rep., Ministry of Environments and Forests, Government of India, 2007. 17055

Jones, A., Thomson, D. J., Hort, M. C., and Devenish, B.: The UK Met Office's next-generation atmospheric dispersion model, NAME III, in: Air Pollution Modeling and Its Application XVII, EDITED BY: Borrego, C. and Norman, A.-L., Springer, New York, USA, 580–589, 2007. 17061

JRC/PBL: Joint Research Centre of the European Commission (JRC)/Netherlands Environmental Assessment Agency (PBL), Emission Database for Global Atmospheric Research (EDGAR), release version 4.2, 2011. 17068

Levin, I., Naegler, T., Heinz, R., Osusko, D., Cuevas, E., Engel, A., Ilmberger, J., Langenfelds, R. L., Neininger, B., Rohden, C. V., Steele, L. P., Weller, R., Worthy, D. E., and Zimov, S. A.: The global SF_6 source inferred from long-term high precision atmospheric measurements and its comparison with emission inventories, Atmos. Chem. Phys., 10, 2655–2662, doi:10.5194/acp-10-2655-2010, 2010. 17056

Manning, A. J., Ryall, D. B., Derwent, R. G., Simmonds, P. G., and O'Doherty, S.: Estimating European emissions of ozone-depleting and greenhouse gases using observations and a modeling back-attribution technique, J. Geophys. Res., 108, 4405, doi:10.1029/2002JD002312, 2003. 17061

Manning, A. J., O'Doherty, S., Jones, A. R., Simmonds, P. G., and Derwent, R. G.: Estimating UK methane and nitrous oxide emissions from 1990 to 2007 using an inversion modeling approach, J. Geophys. Res., 116, D02305, doi:10.1029/2010JD014763, 2011. 17061

Miller, B. R., Weiss, R. F., Salameh, P. K., Tanhua, T., Greally, B. R., Mühle, J., and Simmonds, P. G.: Medusa: a sample preconcentration and GC/MS detector system for in situ measurements of atmospheric trace halocarbons, hydrocarbons, and sulfur compounds., Anal. Chem., 80, 1536–45, doi:10.1021/ac702084k, 2008. 17059

Morrison, N. L. and Webster, H. N.: An assessment of turbulence profiles in rural and urban environments using local measurements and numerical weather prediction results, Bound.-Lay. Meteorol., 115, 223–239, doi:10.1007/s10546-004-4422-8, 2005. 17061

Niemeyer, L. and Chu, F.: SF_6 and the atmosphere, IEEE T. Electr. Insul., 27, 184–187, doi:10.1109/14.123455, 1992. 17056

O'Doherty, S., Cunnold, D. M., Manning, A., Miller, B. R., Wang, R. H. J., Krummel, P. B., Fraser, P. J., Simmonds, P. G., McCulloch, A., Weiss, R. F., Salameh, P., Porter, L. W., Prinn, R. G., Huang, J., Sturrock, G., Ryall, D., Derwent, R. G., and Montzka, S. A.: Rapid growth of hydrofluorocarbon 134a and hydrochlorofluorocarbons 141b, 142b, and 22 from Advanced Global Atmospheric Gases Experiment (AGAGE) observations at Cape Grim, Tasmania, and Mace Head, Ireland, J. Geophys. Res., 109, D06310, doi:10.1029/2003JD004277, 2004. 17061

Panday, A. K. and Prinn, R. G.: Diurnal cycle of air pollution in the Kathmandu Valley, Nepal: observations, J. Geophys. Res., 114, D09305, doi:10.1029/2008JD009777, 2009. 17069

Parker, R., Boesch, H., Cogan, A., Fraser, A., Feng, L., Palmer, P. I., Messerschmidt, J., Deutscher, N., Griffith, D. W. T., Notholt, J., Wennberg, P. O., and Wunch, D.: Methane observations from the Greenhouse Gases Observing SATellite: comparison to ground-based TCCON data and model calculations, Geophys. Res. Lett., 38, L15807, doi:10.1029/2011GL047871, 2011. 17056, 17057

Pathak, H., Li, C., and Wassmann, R.: Greenhouse gas emissions from Indian rice fields: calibration and upscaling using the DNDC model, Biogeosciences, 2, 113–123, doi:10.5194/bg-2-113-2005, 2005. 17055, 17067

Patra, P. K., Houweling, S., Krol, M., Bousquet, P., Belikov, D., Bergmann, D., Bian, H., Cameron-Smith, P., Chipperfield, M. P., Corbin, K., Fortems-Cheiney, A., Fraser, A., Gloor, E., Hess, P., Ito, A., Kawa, S. R., Law, R. M., Loh, Z., Maksyutov, S., Meng, L., Palmer, P. I., Prinn, R. G., Rigby, M., Saito, R., and Wilson, C.: TransCom model simulations of CH_4 and related species: linking transport, surface flux and chemical loss with CH_4 variability in the troposphere and lower stratosphere, Atmos. Chem. Phys., 11, 12813–12837, doi:10.5194/acp-11-12813-2011, 2011. 17068

Prinn, R. G., Weiss, R. F., Fraser, P. J., Simmonds, P. G., Cunnold, D. M., Alyea, F. N., O'Doherty, S., Salameh, P., Miller, B. R., Huang, J., Wang, R. H. J., Hartley, D. E., Harth, C., Steele, L. P., Sturrock, G., Midgley, P. M., and McCulloch, A.: A history of chemically and radiatively important gases in air deduced from ALE/GAGE/AGAGE, J. Geophys. Res., 105, 17751–17792, doi:10.1029/2000JD900141, 2000. 17056, 17058, 17059, 17060

Ravishankara, A. R., Daniel, J. S., and Portmann, R. W.: Nitrous oxide (N_2O): the dominant ozone-depleting substance emitted in the 21st century, Science, 326, 123–125, doi:10.1126/science.1176985, 2009. 17055

Reimann, S., Manning, A. J., Simmonds, P. G., Cunnold, D. M., Wang, R. H. J., Li, J., McCulloch, A., Prinn, R. G., Huang, J., Weiss, R. F., Fraser, P. J., O'Doherty, S., Greally, B. R., Stemmler, K., Hill, M., and Folini, D.: Low European methyl chloroform emissions inferred from long-term atmospheric measurements., Nature, 433, 506–508, doi:10.1038/nature03220, 2005. 17061

Rigby, M., Prinn, R. G., Fraser, P. J., Simmonds, P. G., Langenfelds, R. L., Huang, J., Cunnold, D. M., Steele, L. P., Krummel, P. B., Weiss, R. F., O'Doherty, S., Salameh, P. K., Wang, H. J., Harth, C. M., Mühle, J., and Porter, L. W.: Renewed growth of atmospheric methane, Geophys. Res. Lett., 35, L22805, doi:10.1029/2008GL036037, 2008. 17056

Rigby, M., Mühle, J., Miller, B. R., Prinn, R. G., Krummel, P. B., Steele, L. P., Fraser, P. J., Salameh, P. K., Harth, C. M., Weiss, R. F., Greally, B. R., O'Doherty, S., Simmonds, P. G., Vollmer, M. K., Reimann, S., Kim, J., Kim, K.-R., Wang, H. J., Olivier, J. G. J., Dlugokencky, E. J., Dutton, G. S., Hall, B. D., and Elkins, J. W.: History of atmospheric SF_6 from 1973 to 2008, Atmos. Chem. Phys., 10, 10305–10320, doi:10.5194/acp-10-10305-2010, 2010. 17056, 17057, 17060, 17065

Ryall, D. B. and Maryon, R. H.: Validation of the UK Met. Office's name model against the ETEX dataset, Atmos. Environ., 32, 4265–4276, doi:10.1016/S1352-2310(98)00177-0, 1998. 17061

Schuck, T. J., Brenninkmeijer, C. A. M., Baker, A. K., Slemr, F., von Velthoven, P. F. J., and Zahn, A.: Greenhouse gas relationships in the Indian summer monsoon plume measured by the CARIBIC passenger aircraft, Atmos. Chem. Phys., 10, 3965–3984, doi:10.5194/acp-10-3965-2010, 2010. 17057, 17063, 17067

Thoning, K. W., Tans, P. P., and Komhyr, W. D.: Atmospheric carbon dioxide at Mauna Loa Observatory: 2. analysis of the NOAA GMCC data, 1974-1985, J. Geophys. Res., 94, 8549–8565, doi:10.1029/JD094iD06p08549, 1989. 17066

Tuzson, B., Henne, S., Brunner, D., Steinbacher, M., Mohn, J., Buchmann, B., and Emmenegger, L.: Continuous isotopic composition measurements of tropospheric CO_2 at Jungfraujoch (3580 m a.s.l.), Switzerland: real-time observation of regional pollution events, Atmos. Chem. Phys., 11, 1685–1696, doi:10.5194/acp-11-1685-2011, 2011. 17062

Xiong, X., Houweling, S., Wei, J., Maddy, E., Sun, F., and Barnet, C.: Methane plume over south Asia during the monsoon season: satellite observation and model simulation, Atmos. Chem. Phys., 9, 783–794, doi:10.5194/acp-9-783-2009, 2009. 17056, 17063

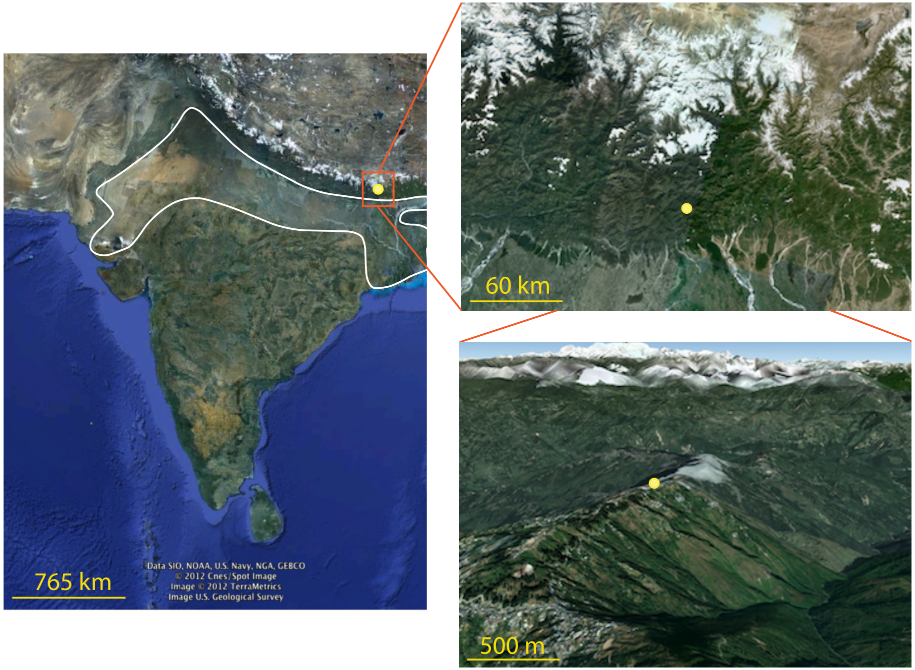

Fig. 1. Location of field site in Darjeeling, India (27°02′ N, 88°15′ E, 2194 m a.g.l., yellow dot) in the Himalayan foothills of Northeast India. The white border shows the approximate location of the Indo-Gangetic plains of India. Images are from Google Earth.

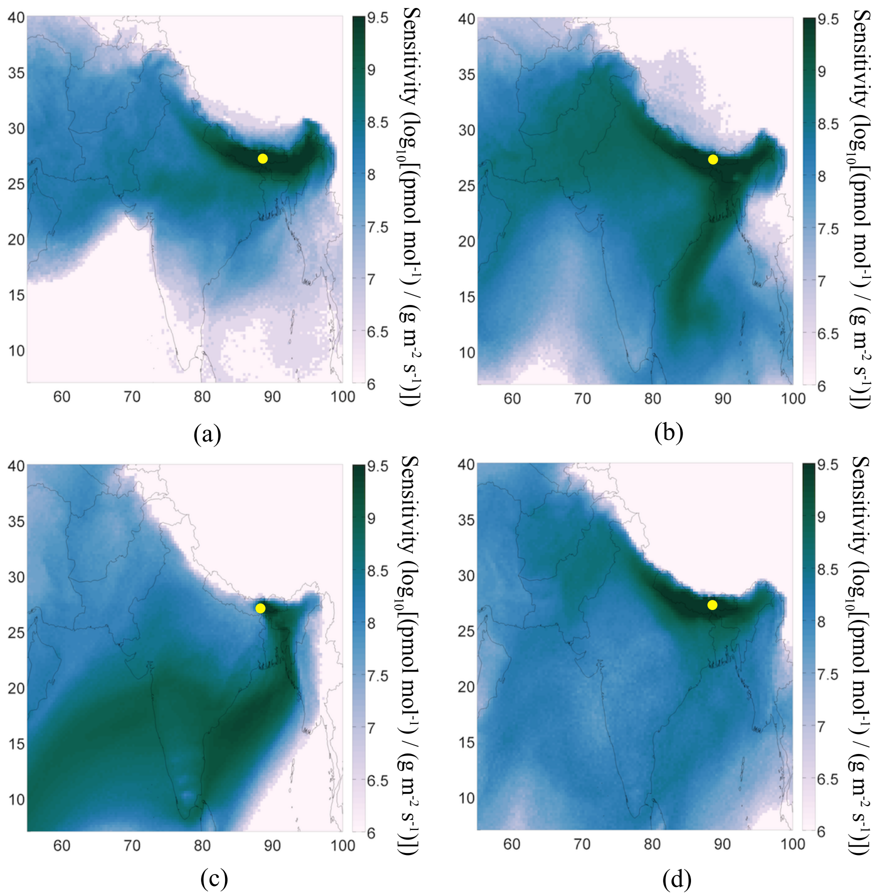

Fig. 2. Monthly median air histories for **(a)** January 2012 **(b)** April 2012 **(c)** July 2012 **(d)** October 2012. Colorbar is a logarithmic scale showing the sensitivity of Darjeeling (yellow dot) mole fractions in pmol mol^{-1} to emissions of any inert gas in g m^{-2} s^{-1}.

Discussion Paper | Discussion Paper | Discussion Paper | Discussion Paper |

ACPD

13, 17053–17085, 2013

Greenhouse gas measurements from Northeast India

A. L. Ganesan et al.

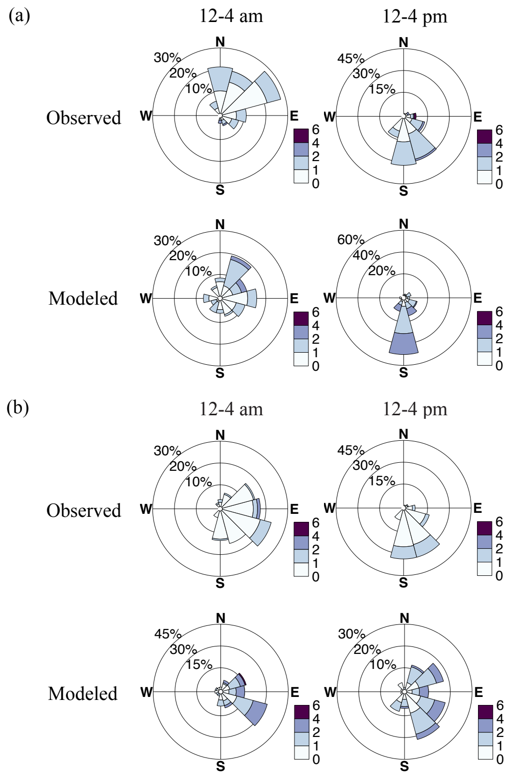

Fig. 3. Wind roses showing percentage of time with given wind direction and speed (colorbar, m s^{-1}). Observed (15 m a.g.l.) and modeled (500 m a.g.l.) wind roses for 12–4 a.m. and 12–4 p.m. for **(a)** January 2012 and **(b)** July 2012.

ACPD
13, 17053–17085, 2013

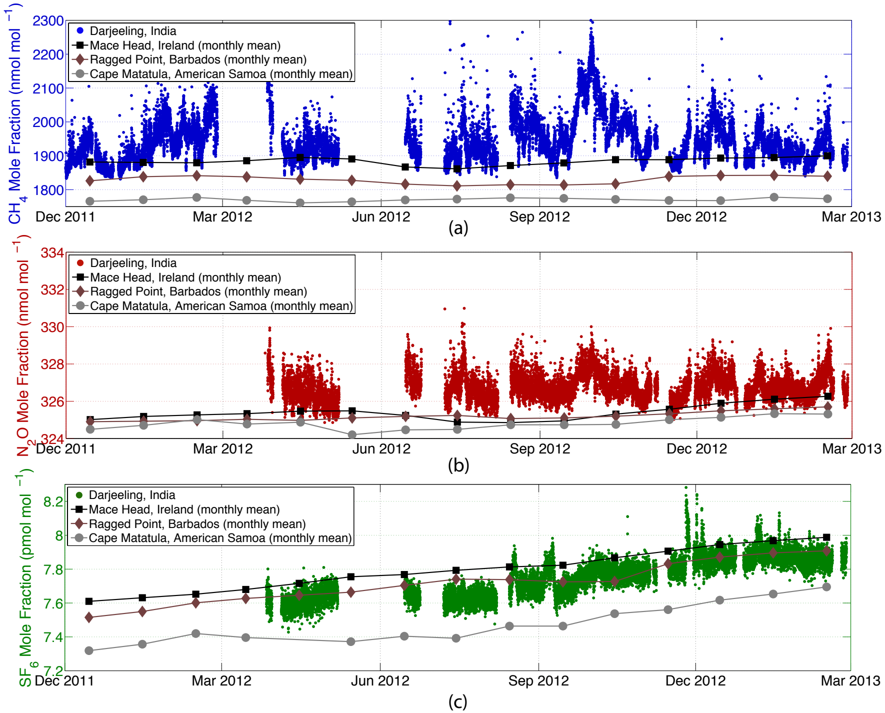

Fig. 4. Measurements of **(a)** CH_4 (blue) **(b)** N_2O (red) and **(c)** SF_6 (green) mole fractions from Darjeeling, India. "Pollution-removed" monthly mean mole fractions from AGAGE measurements at Mace Head, Ireland (black squares), Ragged Point, Barbados (brown diamonds) and Cape Matatula, American Samoa (grey circles) are shown for comparison.

ACPD
13, 17053–17085, 2013

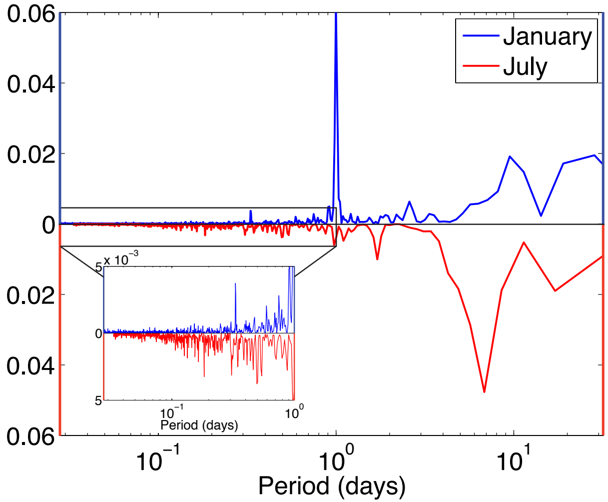

Fig. 5. Power spectrum of January 2012 (blue) and July 2012 (red) CH_4 mole fractions normalized by the total of each month. July is shown as a mirror for visualization.

ACPD
13, 17053–17085, 2013

Title Page
Abstract Introduction
Conclusions References
Tables Figures
◀I ▶I
◀ ▶
Back Close
Full Screen / Esc
Printer-friendly Version
Interactive Discussion

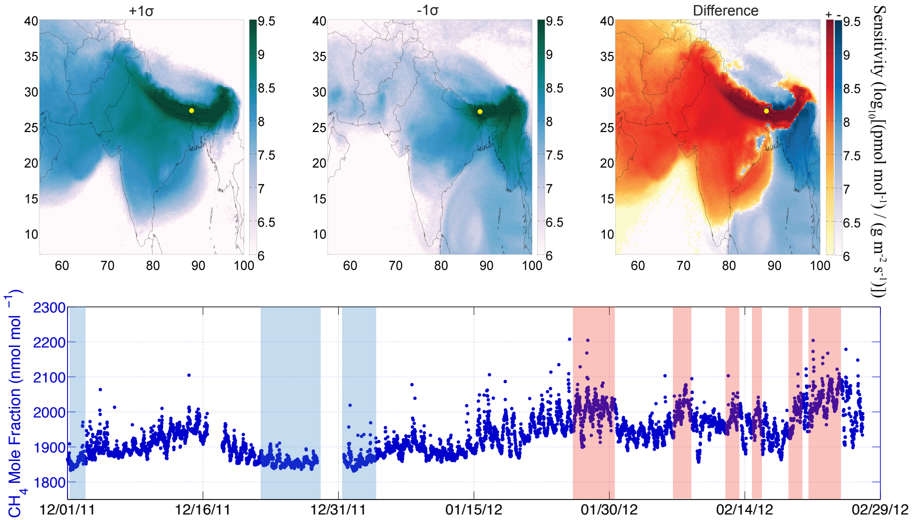

Fig. 6. (Top) Average air histories from Darjeeling (yellow dot) corresponding to CH_4 measurements from December 2011 through February 2012 that are 1σ above the mean of the period after smoothing (top, left), measurements that are 1σ below the mean after smoothing (top, middle) and the difference between the two (top, right). The difference map is shown using two colormaps representing the log value of positive and negative differences, respectively. (Bottom) Mole fractions (unsmoothed) from the period are shown with highlighted portions corresponding to the $+1\sigma$ (red) and -1σ (blue) measurements after smoothing.

ACPD
13, 17053–17085, 2013

Greenhouse gas measurements from Northeast India

A. L. Ganesan et al.

Title Page
Abstract | Introduction
Conclusions | References
Tables | Figures
◀| |▶
◀ ▶
Back | Close
Full Screen / Esc
Printer-friendly Version
Interactive Discussion

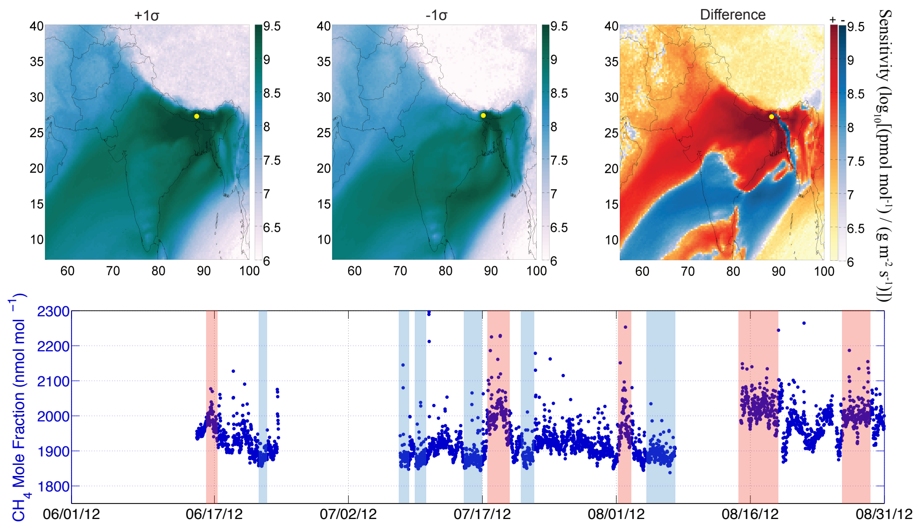

Fig. 7. Same as Fig. 6 but for June 2012 through August 2012.

ACPD
13, 17053–17085, 2013

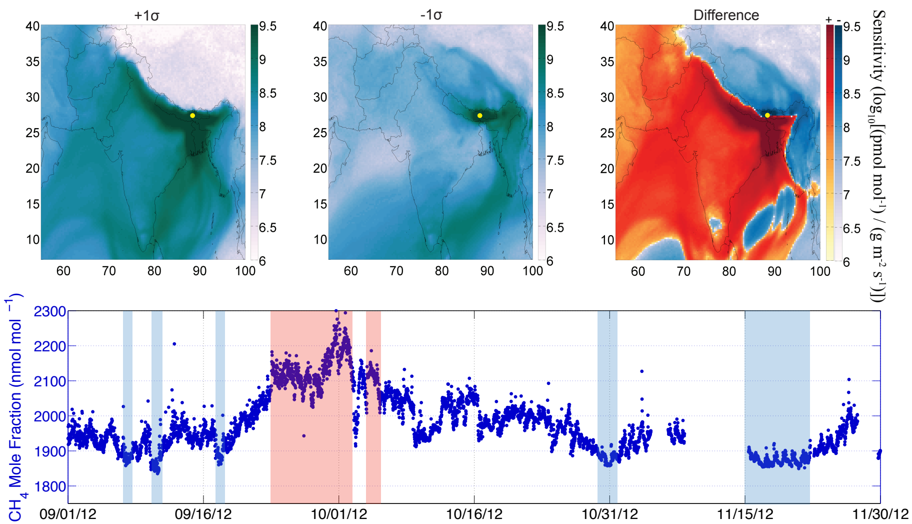

Fig. 8. Same as Fig. 6 but for September 2012 through November 2012.

ACPD
13, 17053–17085, 2013

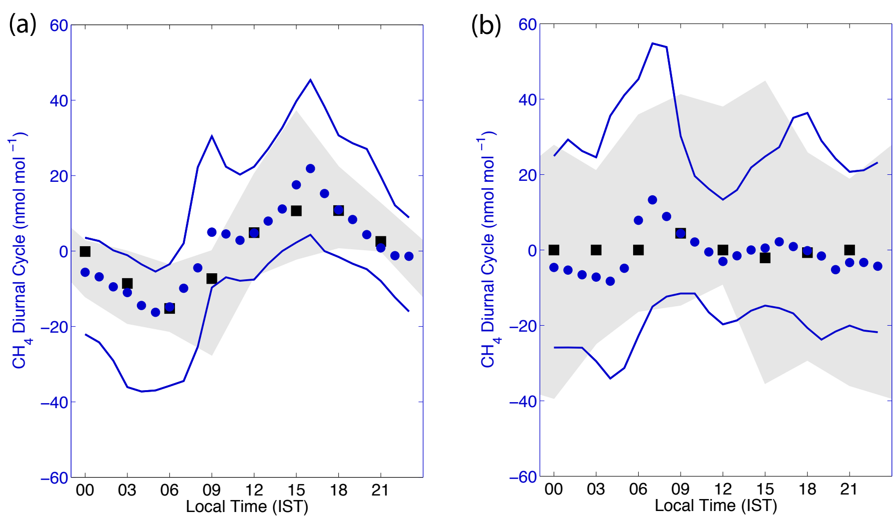

Fig. 9. Median observed CH_4 diurnal cycles (blue circles) and NAME-generated diurnal cycles (black squares) from **(a)** December 2011–February 2012 (winter) and **(b)** June–August 2012 (summer). Solid blue lines and grey shading indicate the 16th and 84th percentile of the observed and modeled values, respectively, from the period.

ACPD
13, 17053–17085, 2013